I. Design a fluorescence microscopy experiment

a) Select fluorophores that are bright and photostable

Choosing fluorophores that a bright and photostable offer many advantages such as allows using less excitation light and acquire longer timelapses with increased temporal resolution. In this experiment, we base on the FPbase database to choose optimal Flurorescent proteins (FPs) for the live cell imaging. In practice, it is necessary to test these FPs in our biological system with specific imaging condition as they may behave very differently in our specific application.

Figure 1 shows the chart of different monomeric FPs, based on Brightness and Bleaching Half-life which represents the photostablity. From this chart we could select a set of potential FPs that could balance well between brightness and photostability. Considering also the separation of excitation and emission peak wavelength, we choose green fluorescent protein **mEGFP** and red fluorescent protein **mCardinal.**

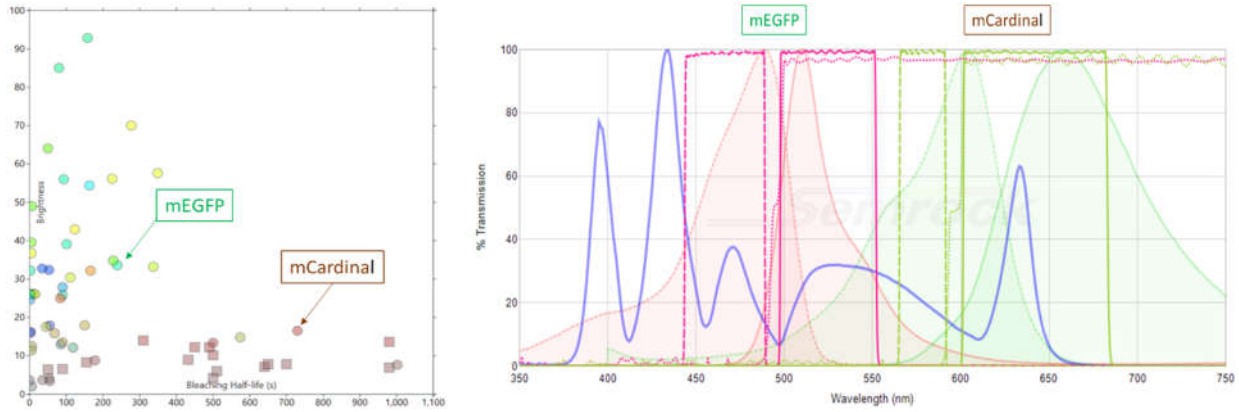

(a) (b)

Figure 1: (a) The chart of different monomeric FPs, based on Brightness and Bleaching Half-life which represents the photostablity. From this chart we could select a set of potential FPs that could balance well between brightness and photostability. Considering also the separation of excitation and emission peak wavelength, we choose green fluorescent protein ***mEGFP*** *and red fluorescent protein* ***mCardinal.*** *(b) Spectral profiles of the two selected FPs and characteristics of corresponding filter sets. Each filter set contains an excitation, a dichroic beam splitter and an emission filter that are selected to optimize the signal to noise ratio.*

The detail properties of the two FPs are summarized in the table below:

Fluorescent Protein	Brightness	Bleaching Half-life (s)	Excitation wavelength (nm)	Emission Wavelength (nm)
mEGFP	33.6	239	488	507
mCardinal	16.53	730	604	659

b) Label mcgillin and the endoplasmic reticulum

In this experiment, cells are cultured and co-transfected with mEGFP (for staining the ER) and mCardinal (for labelling target protein mcgillin) using transient transfection of plasmid DNA technique. By fusing a Fluorescent Protein (FP) gene to the gene that produce target proteins, FPs are incorporated as protein markers. That means the host cell will produce target protein with the fluorescent marker attached. Generally, it's recommended to place gene of interest on the 3' end of the DNA sequence or the C-terminus of the FP fusion.

c) Select filter set

From Semrock database, we choose 2 filter sets, each of which is optimized for a fluorophore: mEGFP and mCardinal. Assume there is a broad-spectrum LED light source (Lumencor SOLA light engine), which produces sufficient wavelengths of photons that is needed to excite the fluorophore. Each filter set contains an excitation, a dichroic beam splitter and an emission filter, particularly:

- An emission filter should be chosen that transmits the peak emission light
- The dichroic beam splitter should be chosen that reflects the excitation and transmits the emission
- Excitation filter should be chosen that transmits the peak excitation wavelengths or large part near the peak excitation wavelength.
- The combination of filters minimizes the noise (crosstalk, autofluorescence, stray excitation light, emission from other fluorophore)

For each fluorophore, we experiment several relevant filter sets and compare their signal to noise ratio under the same illumination condition. For the EGFP, the best filter sets are GFP-4050B, GFP-3035D, GFP-1828A, LED-FITC-A and we choose to use GFP-4050B for analysis. For mCardianl, the best filter sets are mCherry-C, LED-mCherry-A and we choose LED-mCherry-A.

Figure 1(b) shows the spectral profiles of the two selected fluorophores and characteristics of corresponding filter sets.

d) Limit spectral overlap

When imaging with two fluorescent labels simultaneously, there is a concern about signal interference arising from emission overlap by another fluorophore. To limit the overlap, we should consider the following approaches.

Firstly, we should use the bandpass emission filters that are restricted around the peak wavelength of each individual fluorophore. This help to limit the unwanted detection of emission from other fluorophores. Note that as the filter passband size is smaller, the sensitivity could be reduced.

Secondly, even with narrow bandpass filter, emission from one fluorophore can bleed into the detection channel of another. We could mitigate this problem by choosing fluorophores with narrow and well-separated emission spectral profiles. For example, considering the visible range is approximately 300nm (from 400nm to 70nm), two well-separated fluorophores, each has emission spectral profile spanning less than 150nm, will result in desirable signals. However, changing the fluorophores may require the change of filter set.

Lastly, we should consider to reduce concentration of fluorophore in the sample that cause bleed-through and adjust the imaging condition (illumination level, exposure time) that excites that fluorophore, such that the intensity of bleed-through signal is reduced.

e) Set up imaging condition

Our goal in setting imaging condition is to obtain the brightest possible image without saturating any pixels. Here we consider the exposure time, numerical aperture, magnification and illumination intensity.

Exposure time is the length of time the camera collects emission light from the sample, and in live-cell imaging, there are tradeoffs between exposure time, image brightness, and photo-toxicity. Longer exposure time allows more photons to be detected, resulting in increased pixel intensity and thus, a brighter image. However, shorter exposure time is typically required to keep cells functioning and unwanted side effects due to illumination that will complicate the interpretation of the result. Typically, determining the optimal exposure time takes some trial and error on acquiring images.

In the experiment, we use the epi-fluorescence microscope in which the objective also acts as the condenser. Therefore, as the objective magnification increases, the light source image is demagnified by the same amount. So the image brightness is proportional to the fourth power of the objective numerical aperture rather than the square of the numerical aperture as in trans-illumination microscopes. In addition, it is also inversely proportional to the objective magnification squared. Thus, to maximize brightness in fluorescence microscopy image, we will use the highest available numerical aperture objective and the lowest possible magnification necessary to conveniently observe specimen fluorescence.

In fluorescence microscopy, image brightness is also determined by the intensity of illumination besides the quantum yield of the fluorophore and the light-gathering power of the microscope. The greater the intensity of illumination, the greater the fluorescent signal and the brighter the image becomes until all of the fluorophores are saturated. However, illumination should be kept at the lowest level as possible to mitigate photo-bleaching which rapidly degrades fluorescent probes used to stain specimens.

To track the relationship between an imaging condition, for e.g the exposure time, and dynamic range, we can rely on the histogram of intensities in the image collected. Ideally, exposure time should be long enough such that the intensity values span the entire dynamic range, and there are no saturated pixels.

f) Analysis step

Checking the bleed-through:

Before the experiment, single-labeled control to check for any bleed-through of fluorescent signals of the two fluorophores and unlabeled control to check for the auto-fluorescence.

Colocalization analysis:

The contact sites could be detected using fluorescent proteins (FP) targeted to the ER and mcgillin proteins. If they are in contact, the signals from FP would overlap, reporting the presence of contact sites.

Interaction analysis:

By analyzing obtained time-lapse images, we investigate their relative position and direction to each other at different time point or period. Then, we will analyze whether their dynamics is interrelated and disrupted during their movement.

g) Challenges and potential pitfalls and solution

Low brightness and the fading of fluorescent specimens are two major challenges to overcome in fluorescence microscopy imaging.

To increase brightness, exposure time could be long (from seconds to minutes) but there is possibility of over-exposure which results in loss of fine detail and intensity saturation. Thus, the exposure time should be set to the optimal value before measurement.

The inherent weak fluorescence signal is further reduced by photo-bleaching during exposure due to strong illumination and incorrect color reproduction often occurs because of long exposure time. To be able to keep illumination at the minimum level and short exposure time while maintain satisfiable image brightness, we should rely on objectives that have high a numerical aperture as possible, with high transmission values for the used

wavelengths of light. Since the image brightness is proportional to the fourth power of the numerical aperture, these objectives can significantly reduce exposure times and illumination level. In addition, because high numerical aperture objectives have shallower depth of field, they could improve the contrast by reducing the effect of out-of-focus emission. Besides, the total magnification should be kept to a minimum value, as the image intensity is inversely proportional to the square of the magnification.

The use of two fluorescent protein colors with certain degree of spectral overlap can cause cross-talk. This requires the careful selection of fluorescent probes and associated filter sets. Furthermore, natural auto-fluorescence can significantly interfere with green-emitting fluorescence of the probe. One potential solution is using unmixing algorithms to untangle mixed fluorescence signals and resolve the contribution of each fluorophore.

II. Analysis of Interference reflection microscopy images

Interference Reflection Microscopy is a label-free technique that could image single microtubules. However, it is sensitive to sources of noise and non-uniform illumination. So the raw images must be processed to better visualize the sample.

1. Method

Figure 2(A-E) shows the analysis diagram that we experiment to process the raw input and corresponding results after each step. All processing steps are performed by Fiji tool, using macro script for better repetition of the processing pipeline. First of all, the raw image is background-corrected to mitigate uneven illumination and removal of dirt/dust on lenses. The background image was obtained by computing median of a stack of multiple images of a field of view while moving the stage laterally. To do so, a background image was without the objects of interest (microtubules) and also, we can do it after imaging instead of before flowing in the microtubules. To do the background correction, we divide the each of the stack images to the background image, which is done by Image Calculator plugin (or Calculator plus plugin).

The next step is to smooth the stack images by walking average filter, to reduce the noise level. In this technique, a selected number of consecutive frames, particularly 10 frames, will be averaged. In order to maintain the same number of frames, we padded the stack with 9 frames which are the duplicated versions of the last image frame. The main drawback of walking averaging is that it could reduce the temporal resolution, such as when calculating the velocity of the microtubules. Then and from now on, after each processing step, we apply Enhance Contrast function to normalize the gray scale level of every image frame and this normalization is optimal for each frame instead of global normalization for all image frames.

We additionally perform median filter of small kernel size of 3 pixels on each image, which is a non-linear filter for smoothing the image after previous step of running average. We hypothesize it could further reduce the noise while still preserve the edges.

In the subsequent step, we use Fourier filtering to effectively enhance the contrast. It filters out large structures (shading correction) and small structures (smoothing) of specific sizes by Gaussian filtering in Fourier space or the frequency domain. After trial and error attempts, we set the bandpass parameters at 2 and 10 pixels. Finally, after performing normalization, we obtain the final processed image stack which is used for Kymograph analysis.

We also compare the signal to background ratio (SBR) and contrast sensitivity coefficient (CSC) on a frame after applying each proposed technique. Similar to other works in literatures, we compute the microtubule signal as the difference between peak (actually valley) intensity value of microtubule and the average intensity value of the background. Then, the SBR is calculated as the microtubule signal divided by the standard deviation of the background. On the other hand, CSC is calculated as the microtubule signal divided by its standard deviation. We segment the microtubule (object) from background to compute their measurements separately, by using local thresholding based on Sauvola method on the final processed image.

2. Result

Figure 2(A-E) visually demonstrates the improvement of contrast after each step, especially background correction and Fourier filtering steps. Initially, microtubules are hardly visible without background subtraction. The microtubules appear dark against a brighter background. The kymograph on a trajectory of each microtubule could be effectively plotted as shown for example in Figure 2F, by which the speed of expansion of the microtubule could be easily estimated.

Figure 2H compares the intensity profiles of a line scanning across a microtubule after the application of each processing technique. The cross section profile of an example microtubule is measured by taking a line scan perpendicular to the microtubule axis. Figure 2G shows the position of this scan line. In fact, the line width was set to be 50 pixels, which is equal to the microtubule length, such that every point on the cross section profile was an average of all pixels along the microtubule axis. In the profile plot, we could see the increase of signal to surrounding background (note that the microtubules appear dark which is represented by low digital value while the background is bright and is encoded by high digital value). From this plot, the spatial resolution could be estimated by measuring the full width at half maximum. For example, the resolution of the final image, after Fourier filtering is about 0.6 um. Although this value is greater than the value created by previous processing steps, the Fourier filtering technique produce significantly higher contrast.

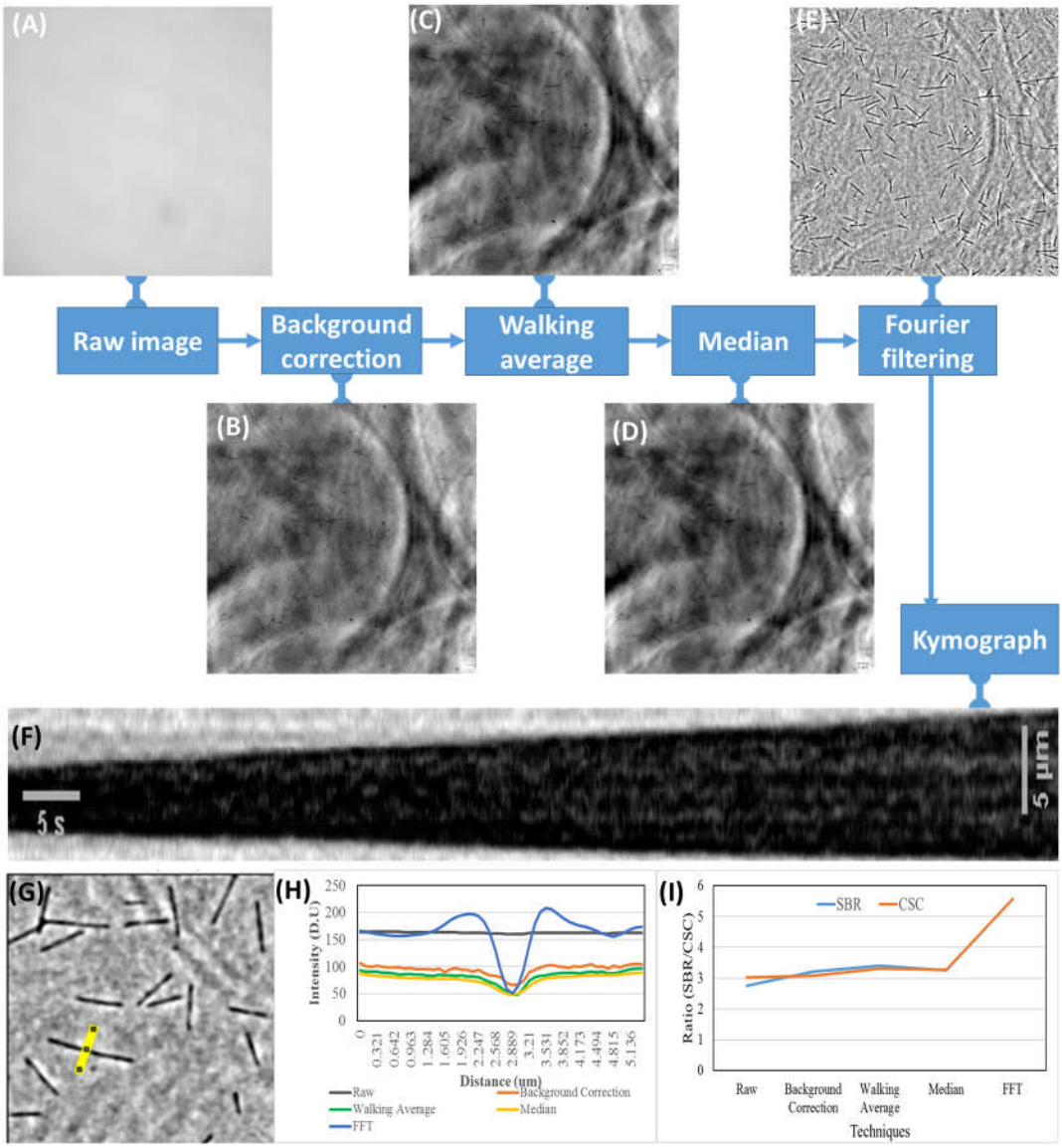

Figure 2. Processing pipeline and comparative evaluation of techniques: (A-E) Processing steps and outputs visually demonstrates the improvement of contrast after each step, especially Fourier filtering in frequency domain; Initially, microtubules are hardly visible without background subtraction; (F) Kymograph on a trajectory of an example microtubule could be effectively plotted to estimate speed of expansion; (G) Position of a scan line perpendicular to the microtubule axis to plot cross-section intensity profiles; (H) Intensity profiles of a line scanning across a microtubule after the application of each processing technique; Every point on the cross section profile was an average of all pixels along the microtubule axis; The spatial resolution could be estimated by measuring the full width at half maximum, which is about 0.6 um after the last step ; (I) Qualitative evaluation the performance gain of processing techniques via the signal to background noise ratio (SBR) and contrast sensitivity coefficient (CSC).

We quantitatively evaluate the performance gain of processing techniques via the signal to background noise ratio (SBR) and contrast sensitivity coefficient (CSC). As can be seen in Figure 2I, the SBR of raw image is 2.76, then it maintains at around 3.3 after using background subtraction, walking average or median filtering. The SBR is double, to 5.56, by the end of the processing pipeline, after the Fourier filtering. We could see a similar trend for CSC ratio, with the starting value of 3.02 and achieving 5.57 after the final processing step.

3. Conclusion and discussion

After applying the proposed technique, the growth and shrinkage of microtubule could be easily observed in the videos and kymographs.

Not all of the filtering technique can improve the signal to background noise ratio or contrast sensitivity coefficient, although they could be widely known with the ability of removing the background noise, particularly the non-linear median filtering. Moreover, the combination of techniques and adjustment of parameters, requiring trial and error attempts.

The intensity normalization should be optimal to every image frame. Otherwise, if there is only a single global dynamic range for all image frame, it should cover the variation of actual dynamic range of all frames (the brightness and contrast of different frames are different).

The SBR and CSC values can be different depending on the specific data. They play the role of a local metric to compare the impact of different processing techniques on a particular image data, rather than to compare with other works. This is because these values also depend on sample preparation as well as the configuration and setting of the imaging system.

In the coming works, other types of filtering and their parameter configuration should be experimented to improve performance. More important, the designed pipeline should be tested on other images and adjusted so that it could work well on different images.

Annex:

The Fiji macro scripts are attached to this report. They include two files: **Processing_pipeline.ijm** and **SBR_CSC.ijm** and should be placed in a working directory together with provided files **IRM-raw.tif** and **translational_background.tif.** The **Processing_pipeline.ijm** should be executed first to process the raw image, and the **SBR_CSC.ijm** executed later to calculate the SBR and CSC ratio.

Acknowledgement and References

Special thank to Dr. Hendricks and Alicia for providing the useful guidance.

References:

1. Exposure time,
https://www.thermofisher.com/ca/en/home/life-science/cell-analysis/cell-analysis-learning-center/molecular-probes-school-of-fluorescence/imaging-basics/capturing-analyzing-your-samples/exposure-times.html
2. Image Brightness
https://www.microscopyu.com/microscopy-basics/image-brightness
3. Choosing a Fluorescent Protein
https://nic.med.harvard.edu/fluorescent-proteins/
4. Choosing the B(right)est Fluorescent Protein: Photostability
https://blog.addgene.org/choosing-the-brightest-fluorescent-protein-photostability
5. A Practical Approach to Choosing the B(right)est Fluorescent Protein
https://blog.addgene.org/a-practical-approach-to-choosing-the-brightest-fluorescent-protein
6. Fluorescence Microscopy Errors
https://www.olympus-lifescience.com/fr/microscope-resource/primer/photomicrography/fluorescenceerrors/
7. Labeling Using Fluorescent Proteins
https://www.thermofisher.com/ca/en/home/life-science/cell-analysis/cell-analysis-learning-center/molecular-probes-school-of-fluorescence/imaging-basics/labeling-your-samples/labeling-using-fluorescent-proteins.html
8. Spectral Imaging and Linear Unmixing
https://www.microscopyu.com/techniques/confocal/spectral-imaging-and-linear-unmixing
9. Friedman, J.R.; Webster, B.M.; Mastronarde, D.N.; Verhey, K.J.; Voeltz, G.K. **ER sliding dynamics and ER-mitochondrial contacts occur on acetylated microtubules.** *J. Cell Biol.* **2010,** *190***, 363–375**
10. Kymograph (time space plot) Plugin for ImageJ,
FMI Basel + A. Seitz, EMBL Heidelberg, 2008/10/31,
https://www.embl.de/eamnet/html/body_kymograph.html
11. Generate and exploit Kymographs,
https://imagej.net/Generate_and_exploit_Kymographs
12. Background correction
https://imagej.net/Image_Intensity_Processing#Background_correction
13. Calculator Plus
https://imagej.nih.gov/ij/plugins/calculator-plus.html
14. MAHAMDEH, M., SIMMERT, S., LUCHNIAK, A., SCHÄFFER, E. and HOWARD, J. (2018), **Label-free high-speed wide-field imaging of single microtubules using interference reflection microscopy.** Journal of Microscopy, 272: 60-66.